



## Algal biosorbent as a basic tool for heavy metals removal; the first step for further applications

Shaimaa T. El-Wakeel<sup>1</sup>, R. M. Moghazy<sup>1\*</sup>, A. Labena<sup>2</sup>, Sh. Husien<sup>3</sup>

<sup>1</sup>National Research Centre (NRC), Water pollution research department, Dokki, Cairo, 12622, Egypt.

<sup>2</sup>Egyptian Petroleum Research Institute (EPRI), Nasr City, Cairo 11727, Egypt.

<sup>3</sup>Faculty of Postgraduate Studies for Advanced Sciences, Beni-Suef University, Beni-Suef, Egypt.

Received 28 March 2019,  
Revised 21 April 2019,  
Accepted 22 April 2019

### Keywords

- ✓ Algal biosorbent,
- ✓ Seed oil,
- ✓ Fatty acids distribution,
- ✓ Gunstone theory,
- ✓ Triglycerides.

[remog81@gmail.com](mailto:remog81@gmail.com)

### Abstract

Great attention has been received for heavy metal removal by algae due to their good performance, low cost and large available quantities. In the present work, Cu<sup>2+</sup> as an example of heavy metal ions was investigated for removal using two macro-algal biomasses *Ulva fasciata* and *Sargassum dentifolium*. The two algal biomasses were collected, washed, dried and grinded using ball mill to get micro- size powders. The prepared biosorbent materials were characterized using FT-IR (Fourier transformed infrared spectroscopy), Transmission Electron Microscopy (TEM) and Dynamic Light Scattering (DLS). Adsorption experiments were performed at different parameters pH, contact time, biosorbents dose and initial Cu<sup>2+</sup> concentration. Furthermore, adsorption isotherms; Langmuir, Freundlich, Dubinin–Radushkevich and modeling kinetics were studied. The biosorption by both *Ulva* and *Sargassum* biosorbent materials achieved at pH 4, 30 and 60 minutes, respectively and 0.5 g/l biosorbent dose. The maximum adsorption capacities, according to Langmuir model, were achieved at 250 and 125 mg/g for *Ulva* and *Sargassum* biosorbent materials, respectively. The adsorption process followed the pseudo-second-order kinetic model. Moreover, this work has represented one of the established papers that direct further work plans toward the application of the algal biosorbent for heavy metals removal.

## 1. Introduction

Releasing of heavy metal ions, generated from industrial processes into water streams, is a dangerous problem due to their non-biodegradable nature and high accumulation and circulation with food chain [1]. Copper ion (Cu<sup>2+</sup>) was considered as one of the most widely used heavy metal in many industries such as electrical and electroplating industries. Using Cu<sup>2+</sup> in high quantity is extremely toxic to living organisms and leads to destroying the ecosystem. Furthermore, it displayed a bad effect on the brain, skin, pancreas, myocardium, and liver [2]. Consequently, many conventional methods were used for Cu<sup>2+</sup> removal such as chemical oxidation or reduction, chemical precipitation and filtration, evaporation, ion exchange, electrochemical treatment and reverse osmosis [3, 4]. However, using conventional methods has exhibited many draw backs such as incomplete metal removal, high energy cost, and production of other waste products or toxic sludge. Therefore, there is an urgent need for eco-friendly wastewater treatment [5, 6] and biosorption technologies at a low cost. biosorption is an accumulation of pollutants on biosorbent material's surface by the help of active sites. Different studies were directed to use agriculture wastes and micro-organisms such as fungi, yeast, cyanobacteria, and algae as biosorbent materials [7, 8].

On the top of all these groups, different forms of algae (micro and macro algal species) such as *Chlorella* sp., *Spirulina* sp., *Sargassum* sp., *Chlamydomonas* sp. were reported with their high ability to bind many industrial pollutants such as heavy metals and dyes with different extents [9, 10]. Those groups were distinguished by their high sorption capacity and ready availability in a practically unlimited quantity. Brown and green macro-algae are the most attractive types that were used by many researchers; although, less number of researchers

used them in small size less than 100  $\mu\text{m}$  [11]. Therefore, the aim of this study was directed to investigate the biosorption behavior of *Sargassum dentifolium* and *Ulva fasciata* for  $\text{Cu}^{2+}$  removal. This work is an initial step for further research and application in different forms such as sheets, membranes, immobilized beads which facilitate harvesting of biosorbent materials after the treatment process. Furthermore, characterization techniques (Fourier Transform-Infrared spectroscopy) FT-IR, Transmission Electron Microscopy (TEM) and Dynamic Light Scattering (DLS) were used. Moreover, isotherm and kinetics modeling were studied in order to understand the nature of the reaction.

## 2. Material and methods

### 2.1. Collection and preparation of algal biosorbents

*Ulva fasciata* and *Sargassum dentifolium* were collected, washed and dried in an oven at 60 °C for 24 h. *Ulva fasciata* was collected from Ras Elbar, the inter-tidal region of the Mediterranean Sea, Egypt and *Sargassum dentifolium* was collected from Ras Gharb, Red sea, Egypt. Afterward, they were identified according to (Aleem 1993) and the dried biomasses were grinded using Planetary Ball Mill, PM 400 “4 grinding stations”[12].

### 2.2. Characterization of the algal-biosorbent materials

FT-IR spectrum of DAB was applied with KBr disc method and spectrum ranges of 400–4000  $\text{cm}^{-1}$  (according to Goband, using Spectrometer Nicolet IS- 10 spectroscopy) and the morphological characteristics of the algal biomasses surface and the pore and particles fractions were examined under a high-resolution transmission electron microscope (JEM-2100 JEOL) [13, 14]. Furthermore, the sizes of the grinded algal biomasses were determined using Dynamic Light Scattering (DLS), using ZETA SIZER-nano series HT-Nano -25, Malven[15].

### 2.3. Adsorption experiments

In order to investigate the ability of the *Sargassum dentifolium* and *Ulva fasciata* biosorbent-materials to remove  $\text{Cu}^{2+}$  from the aqueous solutions, batch experiments were conducted by contacting  $\text{Cu}^{2+}$ -solutions with the adsorbent (1 g/l). To determine the effect of the contact time on the metal adsorption, the prepared samples were shaken at 160 rpm, collected at different time intervals from (5 -120 min), then filtered and analyzed for metal concentration by Inductively Coupled Plasma-Optical Emission Spectrometry (ICP-OES 5100, Agilent, USA). Furthermore, in order to investigate the effect of the initial pH on the removal efficiency, the pH of the aqueous metal solution was varied from 2 - 5.5 at an initial  $\text{Cu}^{2+}$  concentration of 10 mg/l. There are no experiments were done over a pH of 5.5 to avoid the precipitation of  $\text{Cu}^{2+}$  hydroxides. The effect of the biosorbent dose on the adsorption efficiency was determined by varying the biosorbent dose in the range of (0.05 - 1 g/l).

### 2.4. Adsorption isotherms

The description of the sorption equilibrium between the biosorbent materials and the adsorbate was applied using Langmuir, Freundlich, and Dubinin–Radushkevich models, The amount of adsorbed  $\text{Cu}^{2+}$  (mg/g) at equilibrium ( $q_e$ ) was calculated from the mass balance expression given by:

$$q_e = \frac{(C_0 - C_e)}{m} v \quad \dots\dots (1)$$

Where,  $C_0$  and  $C_e$  are the liquid phase concentrations (mg/l) of Cu (II) at an initial and at equilibrium, respectively.  $V$  is the solution volume (L) and  $m$  is the biosorbent material mass (g). The interaction between the adsorbates and the biosorbent materials was described by theoretical isotherm equations in order to optimize its use.

#### 2.4.1. Freundlich isotherm

The Freundlich equation predicted that the adsorption occurs on heterogeneous surfaces and the adsorption capacity is related to the concentrations of metal ion and represented by Eq.

$$\log q_e = \log K_F + \frac{1}{n} \log C_e \quad \dots\dots (2)$$

Where  $C_e$  (mg/l) and  $q_e$  (mg/g) are defined as the equilibrium concentration and amount of metal adsorbed at equilibrium.  $k_F$  and  $n$  expressed the Freundlich constant related to the capacity of adsorption and intensity of adsorption, respectively. When the values of  $(1/n)$  get closer to zero, the surface became more heterogeneous whereas when values were less than unity, the reaction followed the chemisorption reaction.

#### 2.4.2. Langmuir isotherm

Langmuir model is a theoretical model for monolayer adsorption onto a surface with a finite number of equal sites. The general Langmuir equation is as follows:

$$\frac{C_e}{q_e} = \frac{1}{bq_{max}} + \frac{C_e}{q_{max}} \dots \dots \dots (3)$$

Where  $q_{max}$  (mg/g) and  $b$  are Langmuir constant associated with the maximum value of the adsorption capacity and binding energy respectively;

#### 2.4.3. Dubinin–Radushkevich isotherm (DR)

DR isotherm model explained the adsorption mechanism onto a heterogeneous surface and represented in the equation:

$$\ln q_e = \ln q_{max} - \beta \varepsilon^2 \dots \dots \dots (4)$$

Where,  $\beta$  is a constant related to mean free energy ( $\text{mol}^2/\text{kJ}^2$ ), and  $\varepsilon$  representing Polanyi potential, which can be calculated from

$$\varepsilon = RT \ln \left( 1 + \frac{1}{C_e} \right) \dots \dots \dots (5)$$

The isotherm was applied to determine if the adsorption of the metal ions occurs through a physical or a chemical reaction by calculating its mean free energy,  $E$  ( $\text{kJ mol}^{-1}$ ) per molecule of adsorbate by the Eq:

$$E = \frac{1}{\sqrt{-2\beta}} \dots \dots \dots (6)$$

#### 2.5. Kinetic studies

Kinetic studies for  $\text{Cu}^{2+}$  adsorption were carried out to investigate the mechanism of the reaction. The adsorption kinetics processes were done through the adsorption experiments at different time intervals (5 - 120) and metal concentration (10 mg/l) at room temperature.

The experimental data were analyzed using Lagergren's pseudo-first order and pseudo-second order kinetic models as expressed by the following two equations:

$$\log(q_e - q_t) = \log q_e - \frac{K_1 t}{2.303} \dots \dots \dots (7)$$

The pseudo-second kinetic model is based on experimental information of solid phase sorption and applied to heterogeneous systems and the sorption capacity is proportional to the sorbent active sites number.

$$\frac{t}{q_t} = \frac{t}{K_2 q_e^2} + \frac{t}{q_e} \dots \dots \dots (8)$$

Where  $q_e$  is the equilibrium adsorption capacity (mg/g),  $q_t$  is the adsorption capacity at time  $t$  (mg/g),  $k_1$  ( $\text{min}^{-1}$ ),  $k_2$  ( $\text{g}/\text{mg} \cdot \text{min}$ ) are the adsorption rate constants.

### 3. Results and discussions

#### 3.1. Biosorbents characterizations

Different techniques were used to characterize the biosorbent materials in order to identify the nature of the biomasses and interpreted as follows:

##### 3.1.1. FT-IR spectrum analysis

*Ulva fasciata* biosorbent material was shown different FT-IR spectrum (see Fig 1a) that displayed different functional groups appeared at different beaks;  $3420 \text{ cm}^{-1}$  refer to (-OH and -NH) and  $2920 \text{ cm}^{-1}$  represented (aliphatic C-H). Furthermore,  $1638 \text{ cm}^{-1}$  was (carbonyl  $-\text{HC}=\text{O}$ ,  $\text{R}_2\text{C}=\text{O}$ ),  $1389$  and  $1351 \text{ cm}^{-1}$  were (stretching of amides C-N, and N-H) from proteins. As well as, the band that appeared at  $1248 \text{ cm}^{-1}$  stated (- $\text{SO}_3$ ) group, and  $1031 \text{ cm}^{-1}$  [-C-O (alcohol)]. Finally,  $883$  and  $667 \text{ cm}^{-1}$  peaks proved the appearance of ( $\text{H}_2\text{PO}_4^-$  or  $\text{PO}_4^-$ ).

On the other hand, the FT-IR spectral analysis of *Sargassum dentifolium* biosorbent (see Fig 1b) display bands at  $3447 \text{ cm}^{-1}$  (-OH and -NH),  $2924 \text{ cm}^{-1}$  (aliphatic -CH),  $1620$  and  $1427 \text{ cm}^{-1}$  (carbonyl  $-\text{HC}=\text{O}$ ,  $\text{R}_2\text{C}=\text{O}$ ),  $1259 \text{ cm}^{-1}$  (- $\text{SO}_3$ ),  $1033 \text{ cm}^{-1}$  [-C-O (alcohol)], and  $883$  &  $667 \text{ cm}^{-1}$  ( $\text{H}_2\text{PO}_4^-$  or  $\text{PO}_4^-$ ).

### 3.1.2. Dynamic Light Scattering (DLS)

The application of dynamic Light Scattering (DLS) was performed to evaluate the particle sizes distribution for *Ulva fasciata* and *Sargassum dentifolium* biosorbent materials (see Fig. 2). The particle size of *Ulva* biosorbent material showed a relatively lower average size of 0.220  $\mu\text{m}$  than for *Sargassum* biosorbent material that exhibits an average size of 0.309  $\mu\text{m}$ . These will give better biosorption efficiency for *Ulva fasciata* biosorbent in comparison to *Sargassum dentifolium* biosorbent which may be attributed to their available surface area.

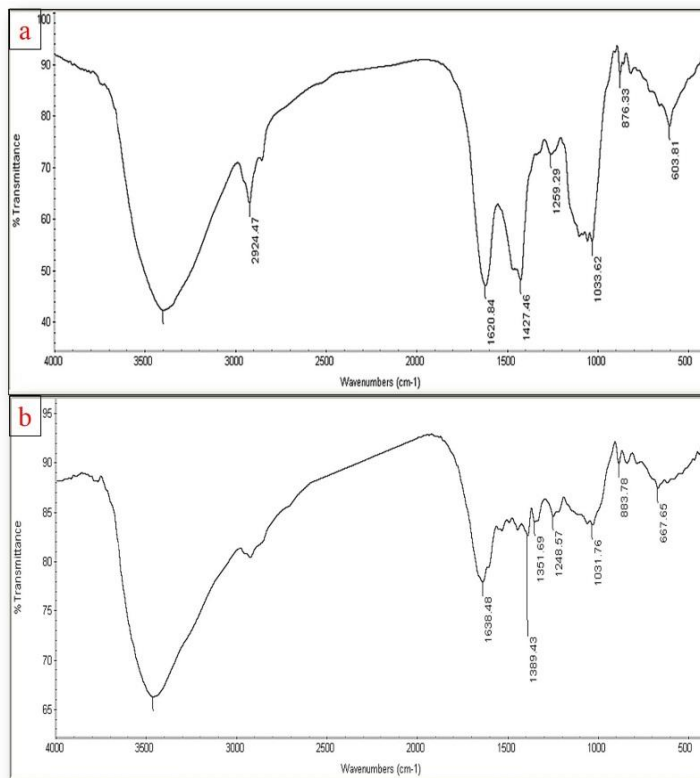


**Fig (1):** FT-IR spectrum of the biosorbent materials (a) *Ulva fasciata* and (b) *Sargassum dentifolium*.

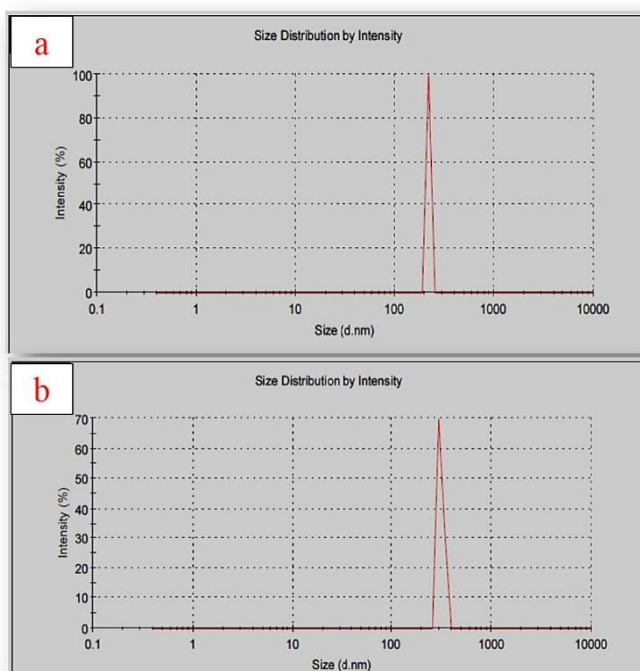


**Fig (2):** DLS the biosorbent materials (a) *Ulva fasciata* and (b) *Sargassum dentifolium*.

### 3.1.3. High resolution Transmission Electron Microscope (TEM)

(TEM) results for the two biosorbent materials; *Ulva fasciata* and *Sargassum dentifolium* were shown in Fig (3a, b). It was proved that the morphology of the biomass material can facilitate the sorption of  $\text{Cu}^{2+}$ , due to the occurrence of an irregular surface of the biosorbent materials that have fractions of micro pores and micro particles. These pores are distributed through the *Ulva fasciata* biosorbent surface than that of *Sargassum dentifolium*. So based on the morphology of the biosorbent, it can be concluded that the biosorbent efficiency of *Ulva fasciata* biosorbent material represented an adequate morphological profile to adsorb metals [16, 17].

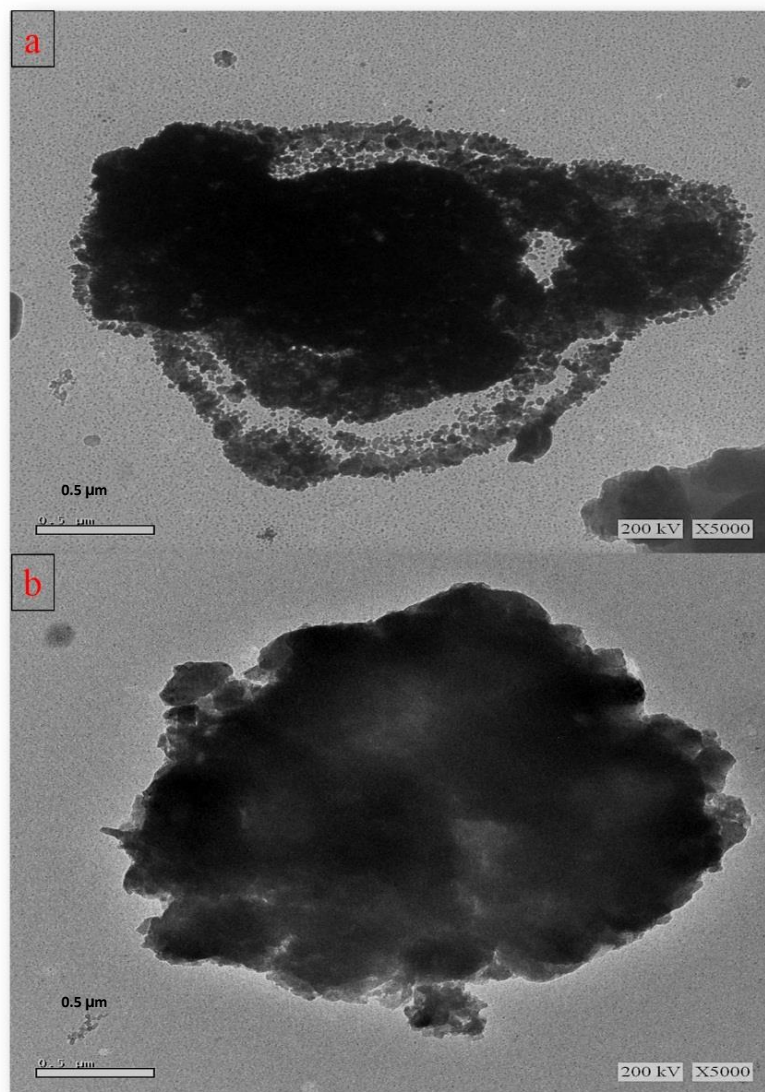


**Fig (3):** TEM micrographs of the biosorbent materials (a) *Ulva fasciata* and (b) *Sargassum dentifolium*.

### 3.2. Determination of $\text{Cu}^{2+}$ removal efficiency at optimum conditions for dye removal

#### 3.2.1. Effect of contact time

The adsorption of  $\text{Cu}^{2+}$  (10 mg/l) on the biosorbent materials at different time intervals were shown in Fig (4 a, b). The  $\text{Cu}^{2+}$  removal efficiency was increased using *Sargassum dentifolium* biosorbent material until the maximum removal of 88 % at 60 min was achieved. Nevertheless, the removal efficiency by *Ulva fasciata* biosorbent material attained 70 % after 30 min. This result may attributed to the high availability of free active sites at the beginning of the reaction then these sites, by increasing  $\text{Cu}^{2+}$  concentration to 20 mg/l, were decreased toward the equilibrium.

In addition, the removal was accomplished in a shorter time for *Ulva* biosorbent material than that of *Sargassum* due to the high availability of free sites in *Ulva* biosorbent material. The removal percentage decreased for both biomass where in *Ulva fasciata* was 63.5 and *Sargassum dentifolium* was 70 %.

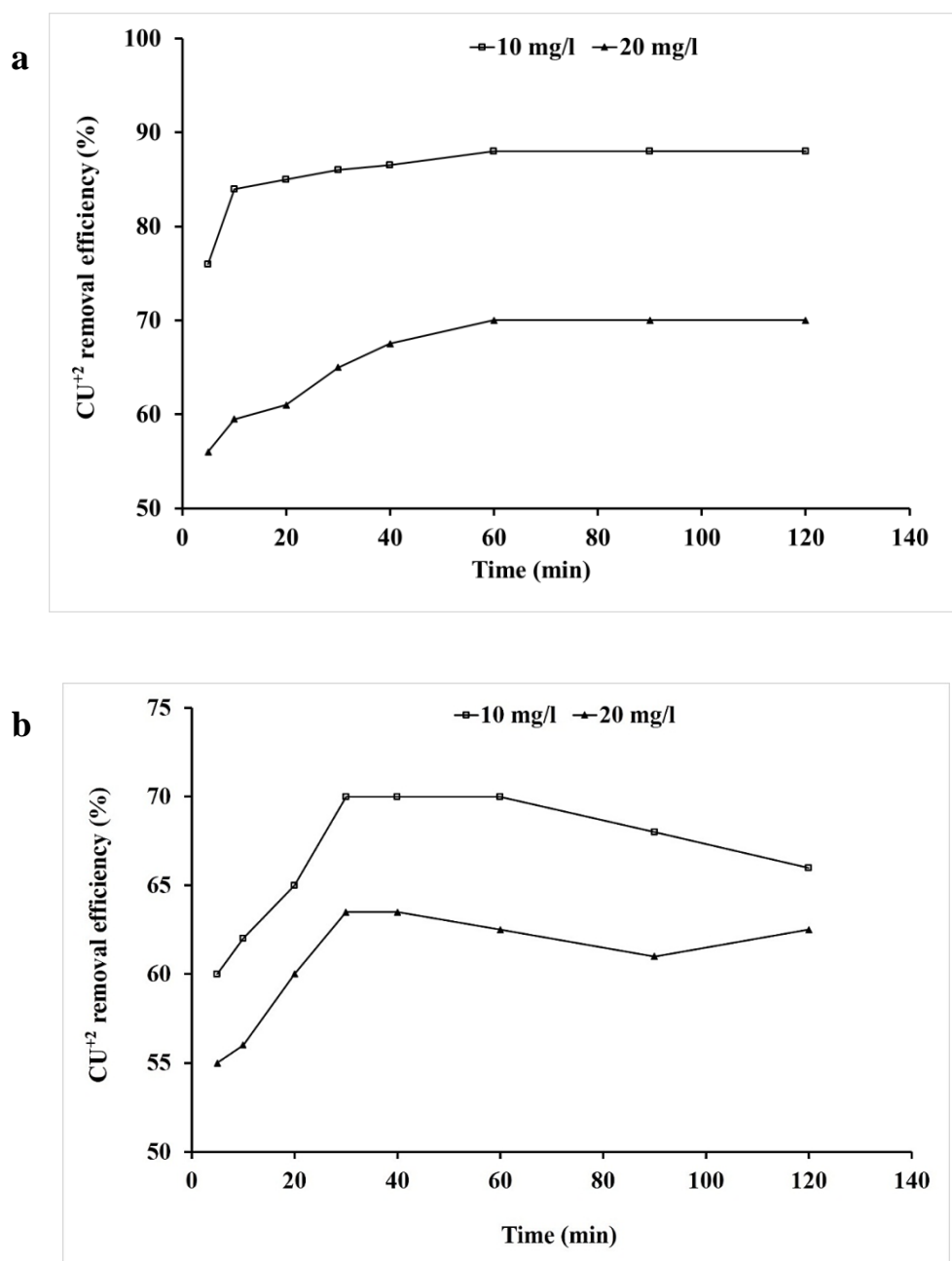


**Fig (4):** Removal percentage of the  $\text{Cu}^{2+}$  ions at different contact time intervals (a) *Ulva fasciata* (b) *Sargassum dentifolium* biosorbent materials (initial  $\text{Cu}^{2+}$  conc. of 10, 20 mg/l, adsorbent dose of 0.5 g/l).

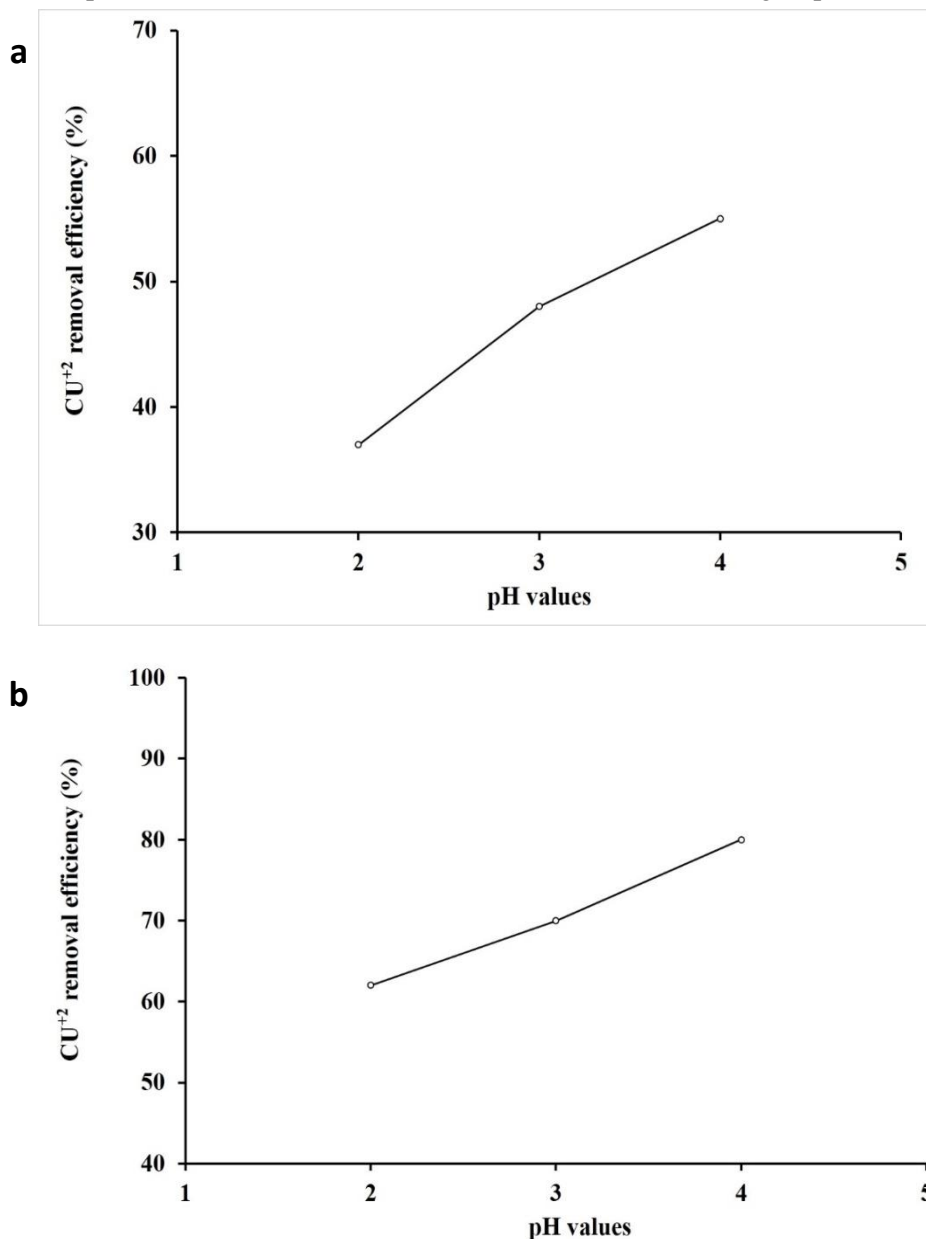
### 3.2.2. Effect of pH

As shown in Fig (5a, b), the adsorption percentage was increased by increasing the pH values from 2–5.3 [18]. On the other hand, at the pH value less than 2, very little amount of  $\text{Cu}^{2+}$  was removed by both types of biosorbent materials. This result may be related to  $\text{Cu}^{2+}$  appearance in the form of the metal ion in the solution, the decreasing in  $\text{H}^+$  ions concentration caused a competition process on the active adsorption sites between  $\text{H}^+$  and  $\text{M}^+$  metal ions [19, 20]. Therefore, the percent of removal of  $\text{Cu}^{2+}$  was increased by increasing the pH value until achieving 5.3 and this result was in a good agreement with the previously reported results. Experiments didn't conduct after 4.5 due to the precipitation of metals hydroxide. These results are in good agreements with the previously studied data [20].

### 3.3. Effect of adsorbent dose and adsorption isotherms

The adsorbent dose was tested over the range of 0.05–1 g/l, with an initial metal concentration of 10 mg/l and a pH value of 4.5 (see Fig 6a, b). The results showed that the  $\text{Cu}^{2+}$  removal efficiency was increased by increasing the biosorbent material dose where a dosage of 0.5 g/l was used. The removal efficiencies of 88 and 71 % for both *Ulva* and *Sargassum* biosorbent materials, respectively were achieved. This may be attributed to a large

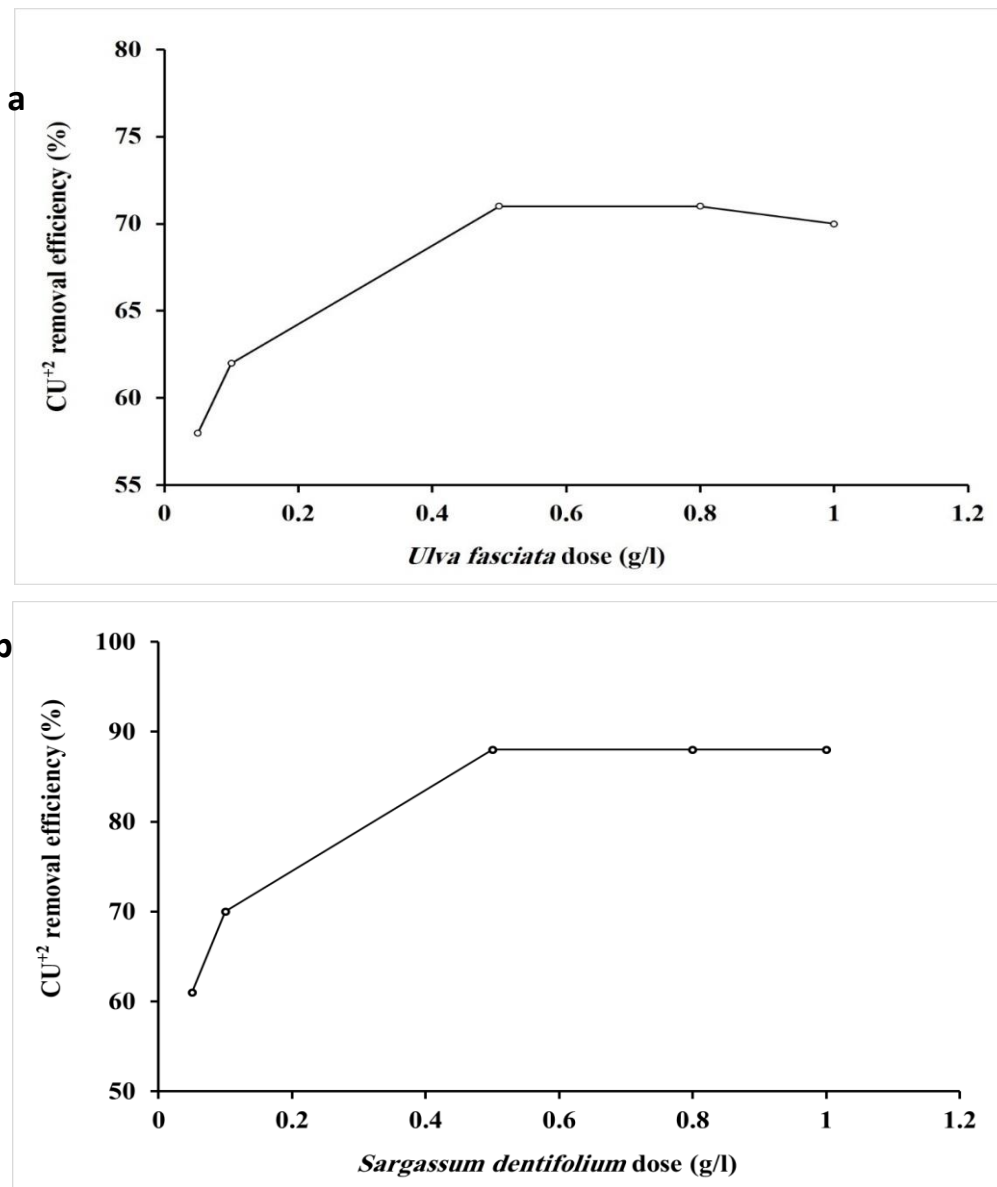
number of functional groups occurred by increasing the dose of algae where the cell wall of the algal cell contains a variety of functional groups such as carboxyl, hydroxyl, amino, sulphonyl, etc. The appearance of these groups in the adsorption experiment improved the removal efficiency due to the ion exchange, micro-precipitation, and complexation occur between the metal ion and the functional groups [21, 22].



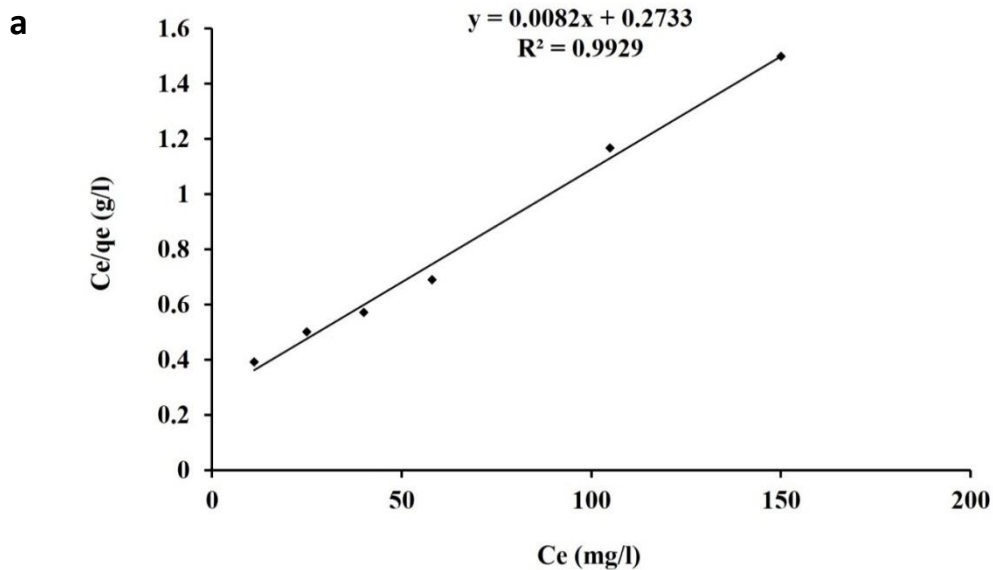
**Fig (5):** Removal percentage of  $\text{Cu}^{2+}$  ions at different pH values by (a) *Ulva fasciata* and (b) *Sargassum dentifolium* biosorbent materials (Initial  $\text{Cu}^{2+}$  conc. of 10 mg/l, adsorbent dose of 0.5 g/l).

### 3.4. Adsorption isotherms

Freundlich and Langmuir isotherm constants were determined from their models as showed in Fig (7, 8a, b). From the displayed results, it was observed that the adsorption behavior of the  $\text{Cu}^{2+}$  on dead algal biomass "*Ulva fasciata* and *Sargassum dentifolium*" biosorbents were in a good agreement with both models, Freundlich and Langmuir as the calculated value of  $R^2$  exhibited more close to 1. By applying the Freundlich equation, the values of  $K_f$  and  $n$  were shown in Table (1). Furthermore, the results revealed that the value of  $1/n$  was less than unity indicating the chemisorption reaction for  $\text{Cu}^{2+}$  ions adsorption [23-25]. The maximum value of the adsorption capacity ( $q_m$ ) and the Langmuir constant  $b$  were estimated from slope and intercept of the linear plot of  $C_e/q_e$  versus  $C_e$  in eq (3), respectively. The maximum value of adsorption capacity ( $q_m$ ) was calculated to be 125 and 250 mg/g by *Ulva* and *Sargassum* biosorbents, respectively. Table (2) demonstrates the comparison between the  $q_{\text{max}}$  of the different algal biosorbents and the present work.



**Fig (6):** Removal percentage of  $\text{Cu}^{2+}$  ions at different doses by (a) *Ulva fasciata* and (b) *Sargassum dentifolium* biosorbent materials (initial conc. of  $\text{Cu}^{2+}$  10 mg/l).



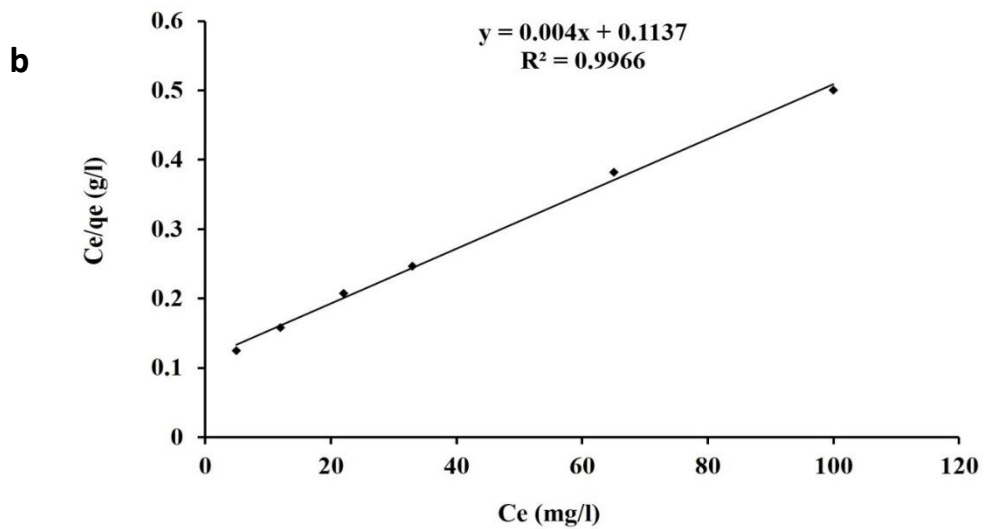


**Fig (7):** Langmuir isotherm plot of  $\text{Cu}^{+2}$  ions adsorption by (a) *Ulva fasciata* and (b) *Sargassum dentifolium* biosorbent materials.

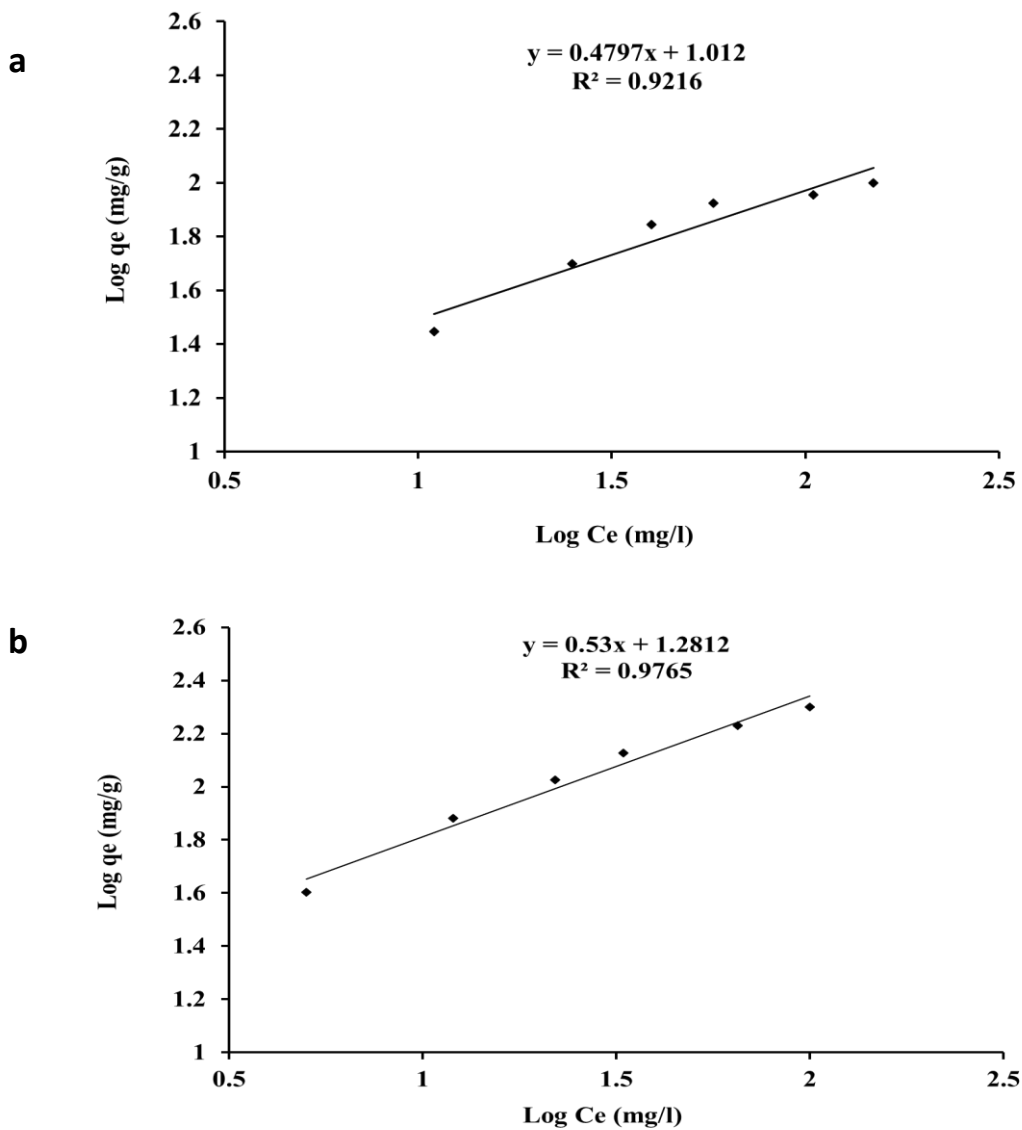


**Fig (8):** Freundlich isotherm plot of  $\text{Cu}^{+2}$  ions adsorption by by (a) *Ulva fasciata* and (b) *Sargassum dentifolium* biosorbent materials.

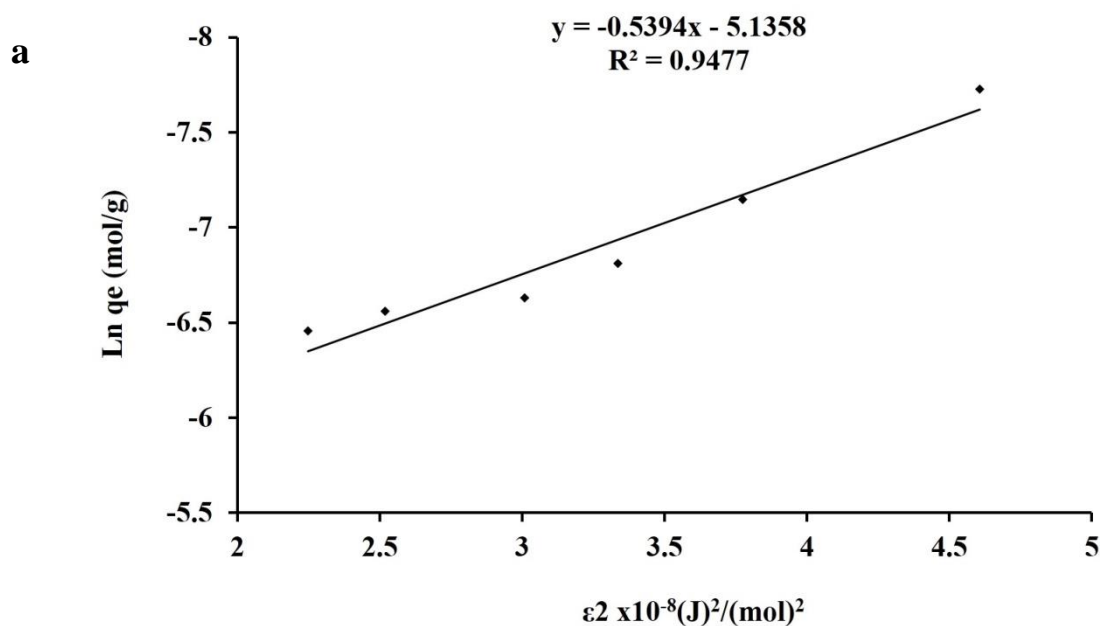
**Table (1):** represented the Isotherm models parameters for Cu<sup>2+</sup> adsorption at room temperature.

	Cu <sup>2+</sup>	
	<i>Sargassum dentifolium</i>	<i>Ulva fasciata</i>
<b>Freundlich isotherm parameters</b>		
<i>l/n</i>	0.53	0.47
<i>K<sub>F</sub></i> (mg/g)	19.1	10.28
<i>R</i> <sup>2</sup>	0.97	0.92
<b>Langmuir isotherm parameters</b>		
<i>q<sub>max</sub></i> (mg/g)	250	125
<i>b</i> (L/mg)	0.03	0.029
<i>R</i> <sup>2</sup>	0.99	0.99
<b>DKR isotherm parameters</b>		
<i>q<sub>max</sub></i> (mol /g)	0.013	0.005
<i>E</i> (KJ/mol)	9.5	9.6
<i>R</i> <sup>2</sup>	0.99	0.95

**Table (2)** represents the comparison of the biosorption performance between different algal biosorbents for Cu (II) ions removal

Species of algae	<i>q<sub>max</sub></i> (mg/g)	References
<i>Cystoseira indicia</i>	<u>103.093</u>	[26]
<i>Sargassum sp</i>	<u>87.05</u>	[27]
<i>Ulva fasciata</i>	<u>125</u>	Present work
<i>Sargassum Sargassum</i>	<u>250</u>	Present work

The value of *R*<sup>2</sup> for the Dubinin-Radushkevich (DR) model (see Fig 9 a, b) was observed to give a good description of the sorption process. The values of the apparent energy of adsorption (*E*) lie between 8 and 16 kJ mol<sup>-1</sup> indication of chemisorption or ion exchange adsorption process. The *E* values estimated were 9.6 and 9.5 kJ/mol *Ulva fasciata* and *Sargassum dentifolium* biosorbents, respectively.



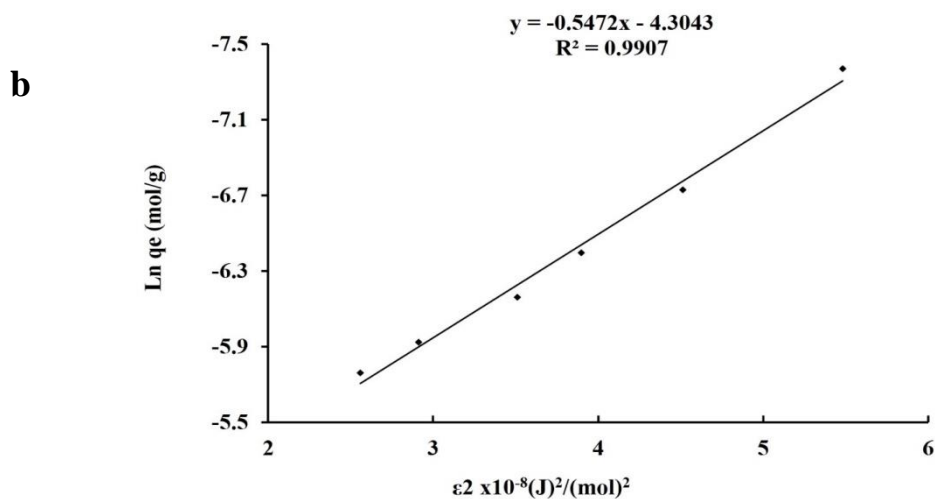


**Fig (9):** Dubinin–Kaganer–Radushkevich (DKR) isotherm plot of  $\text{Cu}^{2+}$  ions adsorption by (a) *Ulva fasciata* and (b) *Sargassum dentifolium* biosorbent materials.

#### Modeling Kinetics

The first-order kinetics plot and its first-order rate constant  $K_f$  value (see Fig 10a, b) were determined from equation (7). The obtained  $R^2$  values were less than 0.95 and the calculated ( $q_e$ ) values didn't agree with the experimental values for both biosorbent materials which revealed that the adsorption does was not follow the pseudo-first-order equation, (see Table 3).

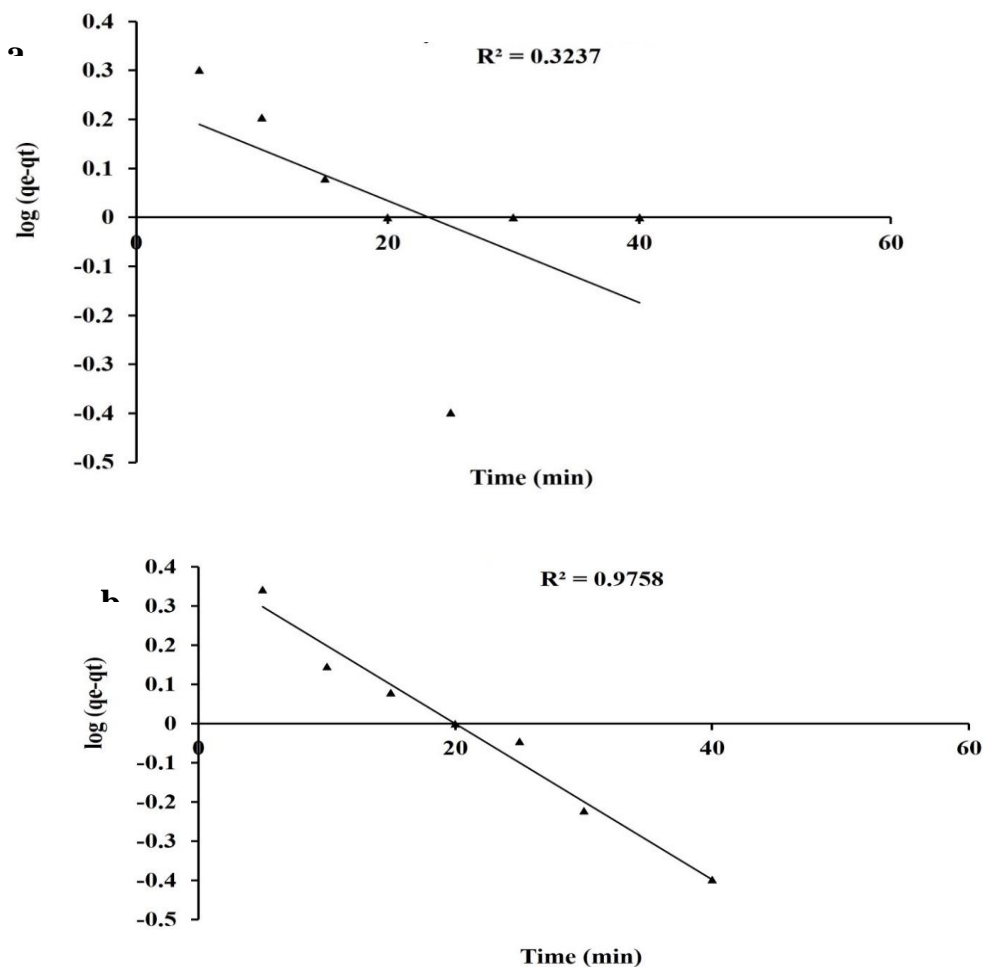


**Fig (10):** Plot of pseudo-first order equation of  $\text{Cu}^{2+}$  ions adsorption by (a) *Ulva fasciata* and (b) *Sargassum dentifolium* biosorbent materials.

**Table 3:** showed the Kinetic parameters of  $\text{Cu}^{2+}$  adsorption at room temperature.

	$\text{Cu}^{2+}$	
	<i>Sargassum dentifolium</i>	<i>Ulva fasciata</i>
<b>Pseudo-first order</b>		
$q_e$ (mg/g)(calculated)	2.5	1.7
$q_e$ (mg/g)(experiment)	17.8	14
$K_1$ ( $\text{min}^{-1}$ )	0.04	0.02
$R^2$	0.95	0.3
<b>Pseudo-second order</b>		
$q_e$ (mg/g) (calculated)	18.18	14.4
$K_2$ (g/mg min)	0.04	0.04
$R^2$	0.99	0.99

Furthermore, by applying the pseudo-second order kinetic model Fig (11a, b), the obtained  $R^2$  values were greater than 0.98 for both biomasses which suggesting that the  $\text{Cu}^{2+}$  adsorption could occur by chemisorption reaction and the calculated ( $q_e$ ) value was very close to the experimental value. Therefore, it could be suggested that the adsorption of  $\text{Cu}^{2+}$  ions follows the pseudo-second order model better than the pseudo-first order one.

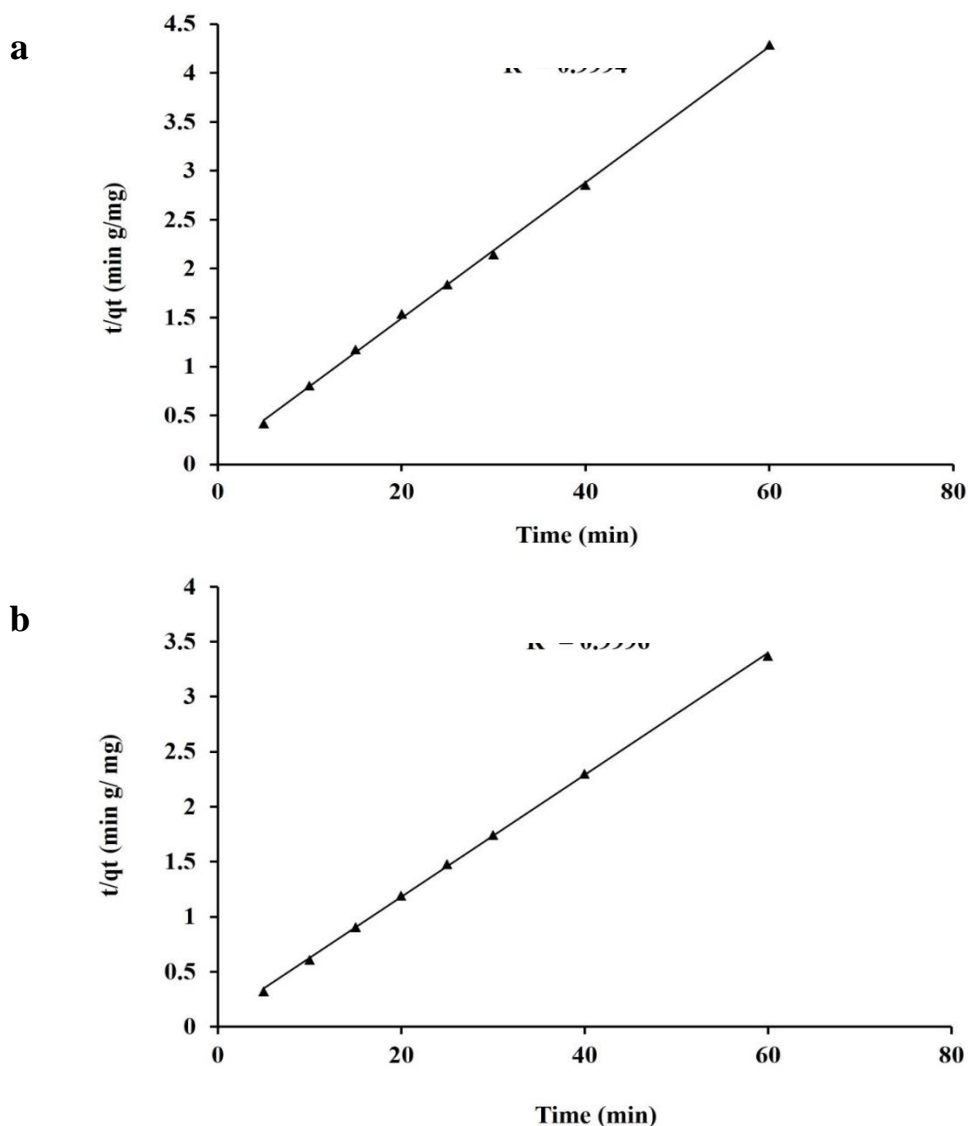


**Fig (11):** Plot of pseudo-second order equation of  $\text{Cu}^{2+}$  ions adsorption by (a) *Ulva fasciata* and (b) *Sargassum dentifolium* biosorbent materials.

## Conclusion and further research

1. *Ulva* and *Sargassum* biosorbent materials were identified according to (Aleem 1993) and recorded as *Ulva fasciata* and *Sargassum dentifolium*.
2. *Ulva fasciata* has successfully achieved a removal efficiency of 70 % at 0.5 g dose after 30 min at pH of 4.0 while *Sargassum dentifolium* a removal efficiency of 88 % at 0.5 g dose took a longer time “60 min.” to remove Cu<sup>2+</sup> from aqueous solution at pH 4.0.
3. Langmuir, Freundlich, and, Dubinin–Radushkevich (DR) isotherms were successfully applicable for both forms of biosorbent materials.
4. The reaction was followed by the pseudo-second order kinetics model.
5. This work is an initial work for future applications in the form of algal-polymer sheets, membranes, beads in order to enhance biosorption efficiency and facilitate harvesting of biosorbents material after treatment process.

## References

1. H. Javadian, M. Ahmadi, M. Ghiasvand, S. Kahrizi, R. Katal, *Journal of the Taiwan Institute of Chemical Engineers*, 44 (2013) 977-989.
2. K. Vijayaraghavan, J. Raj Jegan, K. Palanivelu, M. Velan, *Electronic Journal of Biotechnology*, 7 (2004) 47-54.
3. A. Afkhami, M. Saber-Tehrani, H. Bagheri, *Journal of Hazardous Materials*, 181 (2010) 836-844.
4. S.K. Behzad, A. Balati, M.M. Amini, M. Ghanbari, *Microchimica Acta*, 181 (2014) 1781-1788.
5. H.M. El-Kamah, S.A. Badr, R.M. Moghazy, *Australian Journal of Basic and Applied Sciences*, 5 (2011) 8.
6. H.M. Elkamah, H.S. Doma, S.A. Badr., Saber A El-Shafai, R.M. Moghazy, *Research Journal of Pharmaceutical, Biological and Chemical Sciences*, 7 (2016) 9.
7. M. Sen, M.G. Dastidar, *Iran. J. Environ. Health Sci. Eng. Iranian Journal of Environmental Health Science and Engineering*, 7 (2010) 182-190.
8. S. Ghosh, A. Mondal, A. Paul, *African Journal of Microbiology Research*, 9 (2015) 220-229.
9. R.M. Moghazy, S.M. Abdo, *Res. J. Chem. Environ.*, 22 (2018) 7.
10. R.M. Moghazy, *Water SA*, 45 (2019) 20-28.
11. L. Brinza, C.A. Nygård, M.J. Dring, M. Gavrilescu, L.G. Benning, *Bioresource Technology*, 100 (2009) 1727-1733.
12. A. Aleem, *Egypt. Alexandria*, 55 (1993).
13. D.B. Williams, C.B. Carter, *Transmission Electron Microscopy. A textbook for materials science*, Plenum Press New York, 1996.
14. G. Guibaud, N. Tixier, A. Bouju, M. Baudu, *Chemosphere*, 52 (2003) 1701-1710.
15. B.J. Berne, R. Pecora, *Dynamic light scattering: with applications to chemistry, biology, and physics*, Courier Corporation, 2000.
16. S.A. Badr, A.A. Ashmawy, I.Y. El-Sherif, R.M. Moghazy, *Research Journal of Pharmaceutical Biological and Chemical Sciences*, 7 (2016) 3110-3122.
17. A. El-Sikaily, A. El Nemr, A. Khaled, *Chemical Engineering Journal*, 168 (2011) 707-714.
18. H. Rezaei, *Arabian Journal of Chemistry*, 9 (2016) 846-853.
19. A. Esposito, F. Pagnanelli, F. Veglio, *Chemical Engineering Science*, 57 (2002) 307-313.
20. P. Pavasant, R. Apiratikul, V. Sungkhum, P. Suthiparinyanont, S. Wattanachira, T.F. Marhaba, *Bioresource Technology*, 97 (2006) 2321-2329.
21. V. Gupta, A. Rastogi, *Journal of Hazardous Materials*, 153 (2008) 759-766.
22. B. Volesky, *Water research*, 41 (2007) 4017-4029.
23. Y.-S. Ho, W.-T. Chiu, C.-C. Wang, *Bioresource Technology*, 96 (2005) 1285-1291.
24. J.L. Brasil, R.R. Ev, C.D. Milcharek, L.C. Martins, F.A. Pavan, A.A. dos Santos Jr, S.L. Dias, J. Dupont, C.P.Z. Norena, E.C. Lima, *Journal of Hazardous Materials*, 133 (2006) 143-153.
25. A. Balati, D. Wagle, K.L. Nash, H.J. Shipley, *Applied Nanoscience*, 9 (2019) 19-32.
26. M. Akbari, A. Hallajisani, A. R. Keshtkar, H. Shahbeig, S. A. Ghorbanian, *Journal of Environmental Chemical Engineering*, 3 (2015) 140-149.
27. J. P. Chen, L. Yang, *Industrial & Engineering Chemistry Research*, 44 (2005) 9931-9942.

(2019) ; <http://www.jmaterenvirosnci.com>